Extracellular fluid conductivity analysis by dielectric spectroscopy for *in vitro* determination of cortical tissue vitality

2012 Physiol. Meas. 33 1249

(http://iopscience.iop.org/0967-3334/33/7/1249)

IOP Publishing Physiological Measurement

Physiol. Meas. **33** (2012) 1249–1260 doi:10.1088/0967-3334/33/7/1249

Extracellular fluid conductivity analysis by dielectric spectroscopy for *in vitro* determination of cortical tissue vitality

K F Dobiszewski[1,2,3], M P Deek[1], A Ghaly[1], C Prodan[2] and A A Hill[1]

[1] Federated Department of Biological Sciences, New Jersey Institute of Technology and Rutgers University, Newark, NJ, USA
[2] Department of Physics, New Jersey Institute of Technology, Newark, NJ, USA
[3] Materials Science and Engineering Program, New Jersey Institute of Technology, Newark, NJ, USA

E-mail: aavhill@andromeda.rutgers.edu

Received 1 April 2012, accepted for publication 1 June 2012
Published 27 June 2012
Online at stacks.iop.org/PM/33/1249

Abstract

Brain tissue is extremely metabolically active in part due to its need to constantly maintain a precise extracellular ionic environment. Under pathological conditions, unhealthy cortical tissue loses its ability to maintain this precise environment and there is a net efflux of charged particles from the cells. Typically, this ionic efflux is measured using ion-selective microelectrodes, which measure a single ionic species at a time. In this paper, we have used a bio-sensing method, dielectric spectroscopy (DS), which allows for the simultaneous measurement of the net efflux of all charged particles from cells by measuring extracellular conductivity. We exposed cortical brain slices from the mouse to different solutions that mimic various pathological states such as hypokalemia, hyperkalemia and ischemia (via oxygen-glucose deprivation). We have found that the changes in conductivity of the extracellular solutions were proportional to the severity of the pathological insult experienced by the brain tissue. Thus, DS allows for the measurement of changes in extracellular conductivity with enough sensitivity to monitor the health of brain tissue *in vitro*.

Keywords: dielectric spectroscopy, neural ion flux, extracellular fluid conductivity

(Some figures may appear in colour only in the online journal)

1. Introduction

The maintenance of transmembrane ionic gradients is fundamental for a stable cellular membrane potential (Kettenmann *et al* 1983, Hodgkin and Keynes 1955) and for the viability of neurons (Husted and Reed 1977). The cellular death mechanisms of necrosis and apoptosis are often preceded by a net efflux of ions from cells (Bortner *et al* 1997, Warny and Kelly 1998, Remillard and Yuan 2004). Ionic homeostasis dysfunction may result from, or be exacerbated by, a number of pathological conditions, including cocaine abuse (Du *et al* 2006), hypoxia (Murai *et al* 1997, Müller and Somjen 2000), and traumatic head injury (Takahashi *et al* 1981, Santhakumar *et al* 2003).

Dielectric spectroscopy (DS), a technique that characterizes a medium's impedance as a function of frequency, has been used to investigate a variety of cellular and tissue properties, such as membrane potential (Bot and Prodan 2009), membrane structure and properties (Gheorghiu and Gersing 2002, Di Biasio and Cametti 2011, Ron *et al* 2008), glucose concentration in tissue (Caduff *et al* 2006), and to distinguish between the different cellular death mechanisms (Lee *et al* 2009). DS has also been used to investigate pathology-induced biophysical changes in tissue (Gersing 1998, Egot-Lemaire *et al* 2009, O'Rourke *et al* 2007, Schaefer *et al* 2002). While DS has been used to determine the conductivity of brain tissue (Schmid *et al* 2003) and the dielectric properties of aqueous ionic solutions (Chen and Hefter 2003, Cametti *et al* 2011), we do not know of any previous investigations that have assessed whether a correlation exists between the conductivity of the extracellular fluid surrounding a brain slice and the health of brain tissue.

In this paper, we describe a bio-sensing method to assess, in a relatively noninvasive way, the health of a tissue by measuring the conductivity of electrolytic solutions in which cortical brain tissue slices from CD-1 mice were bathed. We mimic several insults such as hyperkalemia, hypokalemia and oxygen-glucose depravation, using tissue from two age groups of mice: weanling and neonatal. We found that these treatments lead to significant changes in conductivity of the bathing solution surrounding the brains slices, suggesting that DS may be used to measure the viability of brain tissue.

2. Materials and methods

2.1. Experimental solutions

Solutions, with varying concentrations of several key constituents (as detailed in table 1), served as the bathing media for the cortical tissue slices. These solutions were intended to mimic pathological conditions such as hypokalemia, hyperkalemia and oxygen-glucose deprivation (OGD). They were buffered with 5 mM HEPES, and their pH values were adjusted to 7.4 using 1N NaOH or 1M HCl. Osmolarity was adjusted to a measured value of 310 mOsm (using a Wescor Vapro 5600 vapor pressure osmometer) by adding an appropriate concentration of sucrose. All solutions were saturated via an air stone with 100% oxygen, except for the OGD solution, which was saturated with 100% nitrogen.

To better observe ion flux, the ionic concentrations of the solutions were maintained low, thus minimizing the initial conductivity of the solution. Thus, we utilized a total of 10 mM of monovalent cations (K^+ and Na^+) and 10 mM of a monovalent anion (Cl^-). To vary the extracellular K^+ concentrations, an increase in K^+ concentration was matched by an equimolar decrease in Na^+ concentration. While the concentration of sodium in the cerebrospinal fluid (CSF) is approximately 147 mM (Morrison 2008), the majority of transmembrane sodium channels are usually closed at the resting membrane potential, so this low extracellular

Table 1. The ionic composition and glucose content of each experimental solution. Additionally, each solution is buffered by 5 mM of HEPES and contains an appropriate concentration of sucrose such that the measured osmolarity of the solution was about 310 mOsm. Aside from control, each experimental solution had an ionic composition, glucose content, and/or gaseous saturation that could be considered pathological.

Solution	[KCl] (mM)	[NaCl] (mM)	[D-Glucose] (mM)
Control	3	7	15
Severe hypokalemia	0	10	15
Moderate hypokalemia	1	9	15
Hyperkalemia	10	0	15
Oxygen-glucose deprivation	3	7	0

Na^+ level has little influence on membrane potential (van Mil *et al* 2003) and, therefore, should not damage the neural tissue.

2.2. Preparation of cortical tissue samples

Experiments were performed using a slice preparation of the cerebral cortex of CD-1 mice. The Animal Care and Facilities Committee at Rutgers approved this protocol, which is also in accordance with EU directive 86/609/EEC. CD-1 mice were either obtained directly from Charles River Laboratory (Wilmington, MA) or bred from Charles River Laboratory stock. Two experimental age ranges were used: 'neonatal' mice ranged from postnatal day zero (P0) to postnatal day two (P2) and 'weanling' mice ranged from postnatal day 14 (P14) to postnatal day 16 (P16). Mice were anesthetized with isoflurane until the absence of a withdrawal reflex from toe pinch. The mice were decapitated and the whole brain dissected in ice-cold slicing solution containing: 7 mM NaCl, 3 mM KCl, 5 mM HEPES and 15 mM D-glucose. The pH was adjusted to 7.4 with 1N NaOH or 1M HCl and the osmolarity was adjusted to 310 mOsm with sucrose. The excised brain was mounted (with cyanoacrylate glue) to an agar block backing with the dorsal side of the brain facing up. Progressive sections in the coronal plane were made in the rostral-to-caudal direction using a vibrating blade microtome (Leica VT 1200). The brain slices were then incubated for a period of at least 15 min in room temperature saline saturated with 100% O_2.

2.3. Exposure of brain tissue to experimental solutions

In order to supply brain tissue slices with the appropriate gaseous mixture, incubation chambers were constructed from 1.5 mL microcentrifuge tubes. Attempts to oxygenate the tissue via direct flow of gaseous oxygen into the bathing solution resulted in the formation of large bubbles that caused the mechanical disintegration of the tissue slices. Therefore an interface between the oxygen and the bathing solution was required (figure 1). A composite of poly(dimethylsiloxane) (PDMS) (Silgard 184; Dow Corning, Midland, MI, USA) and 1 mm soda glass beads was utilized as this interface. PDMS was chosen as the membrane material because of its excellent oxygen permeability (Hitoshi *et al* 2005) and the reinforcing beads were utilized to support the gas conduit and the PDMS membrane. Gas flow was supplied to the solution through a 30 G subcutaneous needle that was inserted through the side of the microcentrifuge tube such that the tip of the needle came to rest immediately below the surface of the PDMS. To further increase the oxygen saturation of the bathing solution, oxygen was also supplied via a small gauge needle integrated in the cap of the microcentrifuge tube into

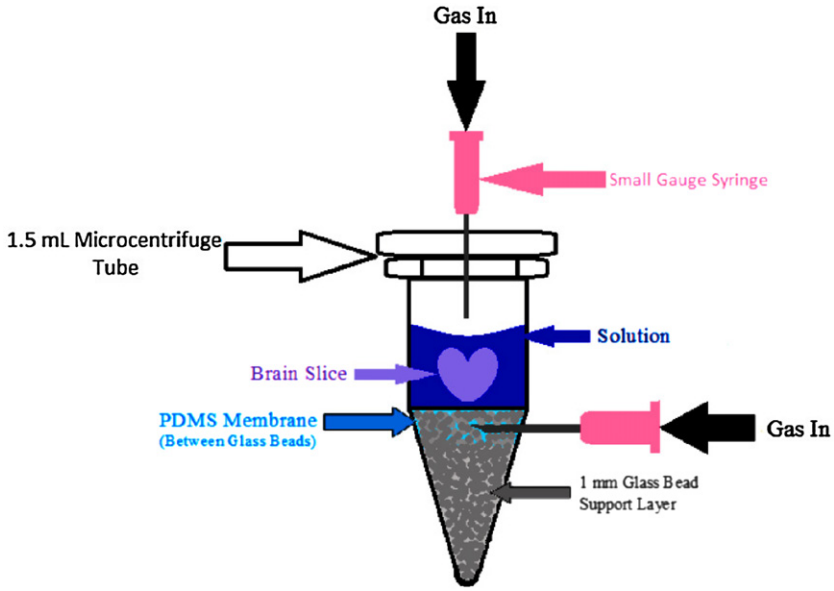

Figure 1. A custom incubation chamber consisting of a 1.5 mL microcentrifuge tube was used to bathe 600 μm thick cortical brain tissue slices in experimental solutions that mimic various pathological conditions. A novel composite material, consisting of 1.0 mm diameter soda glass beads embedded in a polydimethylsiloxane matrix, allowed for adequate supply of experimentally-dictated gas (oxygen or nitrogen) to the tissue slice without causing mechanical trauma to the tissue slice due to its interaction with large gas bubbles.

the airspace just above the bathing solution. A small hole in the cap of the tube enabled the equalization of pressure.

All experiments were performed at room temperature (23 $^\circ$ C). Prior to the exposure of the brain slices to each experimental solution they were washed to rid them of any remnant of the slicing solution. Each slice was transferred to a microcentrifuge tube followed by the removal of all solution via a micropipette. The slice was then immediately washed with 0.2 mL of the experimental solution, which was then removed after 60 s. This step was subsequently repeated. Subsequently, the tissue was transferred to one of the previously described modified incubation tubes. Pure oxygen, or nitrogen in the case of OGD, was supplied at this point. 325 μL of the desired experimental solution (control, hyperkalemia, OGD, etc) was transferred to the modified incubation tube. Concurrently, a 325 μL sample of the experimental solution was collected without exposure to tissue and preserved in order to act as a basis for conductivity change comparison. The tissue was bathed in the experimental solution for 20 min, at which point it was removed from the tissue while the tissue was discarded. The extracellular bathing solution was removed for later analysis while the tissue sample was discarded at this point. Consequently, only the conductivity of the bathing solution was analyzed. The exposed solution and non-exposed solutions were stored at -20° C until analysis by DS occurred.

2.4. Conductivity measurements and analysis

Dielectric spectroscopy, which has previously been shown to successfully probe the conductivity of polyelectrolyte solutions (Bordi *et al* 2004), was utilized to measure the complex conductivity of each solution sample. The electrode system has been previously

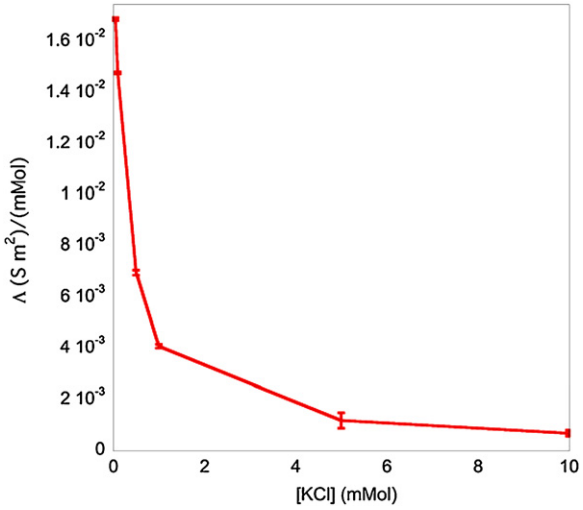

Figure 2. The molar conductivity of a strong electrolyte solution (KCl) with respect to molar concentration is presented as the solid line. Kohlrausch's law theoretically defines the relationship between molar conductivity (Λ) and molar concentration as a power law regression for all strong electrolytes.

described (Dobiszewski *et al* 2011) and shown to successfully measure conductivity. Briefly, the electrode system consisted of two 14 karat gold electrodes held parallel to one another at a precise distance apart. Prior to measurement of each solution, the distance between the electrodes was calibrated using Milli-Q water.

The impedance analyzer (Solartron 1260; Solartron Analytical Hampshire, UK) and electrical circuit (custom) have been previously described by Prodan *et al* (2004) and Bot and Prodan (2009). The complex conductivity function $\sigma = \sigma' + i\omega\,\varepsilon_0\varepsilon$ of the sample can be calculated from the expression for the impedance (Z):

$$Z = \frac{\mathrm{d}\sigma + i\omega\,\mathrm{d}\varepsilon\varepsilon_0}{\sigma^2 A + \omega^2\varepsilon^2\varepsilon_0^2 A} \tag{1}$$

The obtained conductivity spectra were calculated from the experimental (impedance) data by a custom Matlab program utilizing the relationship

$$\sigma(\omega) = \mathbf{Re}\left\{\left(\frac{1}{Z(\omega)}\right)\left(\frac{d}{A\,R}\right)\right\} \tag{2}$$

where d is the distance between the electrodes, A is the surface area of one electrode, ε is the dielectric permittivity of the sample, σ is the conductivity of the sample, R is the experimental resistance and $\omega = 2\,\pi\,\mathrm{f}$, where f is the frequency of the applied signal.

Dielectric spectroscopy measurements were made on each solution from 100 Hz to 1 MHz at a probing voltage of 50 mV. Here we present our analysis of conductivity at 100 Hz, which is within the range used by others (Akhtari *et al* 2006). The conductivity of each solution was calculated via a custom Matlab program. The change in conductivity was defined as the difference between two solutions: a test solution exposed to the tissue slice and a control solution that was not.

2.5. Statistical analysis

Statistical analyses were performed using SigmaPlot v. 11.0 (Systat Software, San Jose, CA). A two-way ANOVA, with experimental condition (control, severe and moderate hypokalemia, hyperkalemia, OGD) and age (neonate versus weanling) as factors, was performed. Where significant main effects of age, experimental condition, or an interaction between the two were found, pair-wise post hoc tests (Holm-Sidak method) were performed for comparison. If a significant interaction was found, main effects were discarded. For all tests, a p value of <0.05 was considered significant. The reported values have been expressed as mean $\pm$ SEM.

3. Results

In order to provide proof that our measurement system was capable of measuring the strong electrolytes likely to be encountered in the extracellular solutions of the brain, we first assessed the molar conductivity of a prototypical strong electrolyte (KCl) with respect to molar concentration; the results are presented in figure 2. Notice that the result presented in this figure follows the power law relationship described by Kohlrausch's law (Coury 1999). Therefore, we deduce that our system can accurately measure the conductivity of strong electrolytes.

The focus of this study was the analysis of the change in conductivity of extracellular solutions subsequent to bath exposure with live cortical tissue. Furthermore, as the brain's response to pathologic conditions can change as a function of age, two distinct age ranges were tested: neonatal and weanling.

Figure 3 represents the conductivity versus frequency corresponding to 'severe hypokalemia' (0 mM $[KCl]_O$; top), control (3 mM $[KCl]_O$; middle) and 'hyperkalemia' (10 mM $[KCl]_O$; bottom). As one can see, for 'severe hypokalemia', the spectrum for the weanling was greater than the spectrum for the neonatal at low frequencies. However, at higher frequencies (above approximately 10 kHz), the spectra for both ages converged and eventually overlapped. For the 'hyperkalemia' condition, this trend was reversed; the spectrum corresponding to the neonates was greater than that of the weanlings at low frequencies. At higher frequencies, the spectra for both age ranges converged and eventually overlapped. The middle graph represents control conditions (3 mM $[KCl]_O$) and was characterized by overlapping spectra for neonates and weanlings at all frequencies.

Figure 4 shows the change in extracellular conductivity of the various experimental solutions after exposure to brain slices. In tissue from weanlings, all three experimental extracellular K^+ concentrations produced statistically significant increases in conductivity compared with the control solution (3 mM KCl). The largest change in conductivity was in response to severe (0 mM $[KCl]_O$) hypokalemia. The increase in conductivity, resulting from moderate (1 mM $[KCl]_O$) hypokalemia was less than the increase in severe hypokalemia. Furthermore, the increase in conductivity was lower in response to hyperkalemia (10 mM $[KCl]_O$) compared to moderate and severe hypokalemia. Therefore, in weanlings as the extracellular potassium concentration was varied there were graded increases in conductivity, with severe hypokalemia leading to the greatest change and hyperkalemia leading to the least change. In response to OGD, there was a greater increase in conductivity compared with the control solution in weanlings. This increase was significantly different from those observed after exposure to moderate hypokalemia and hyperkalemia (figure 4).

In the neonates, all experimental conditions produced statistically significant changes when compared to the control solution (3 mM KCl). However, unlike the weanling data, there was no significant difference between exposures to moderate hypokalemia and severe

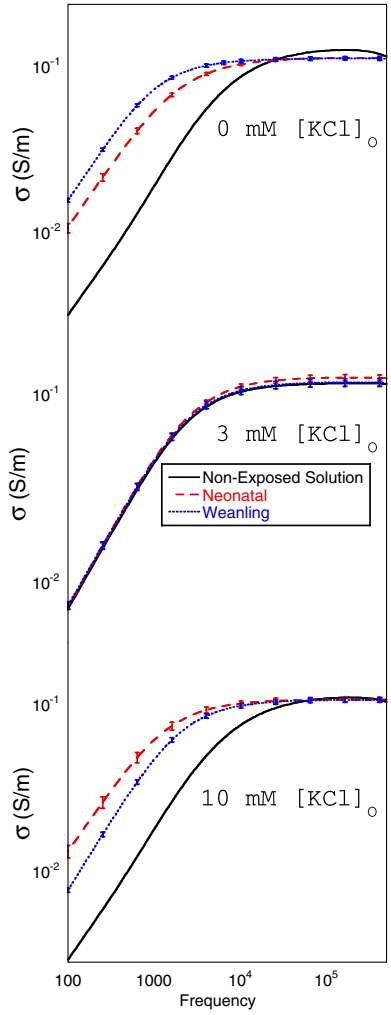

Figure 3. Conductivity with respect to frequency from 100 Hz to 1 MHz for three different extracellular potassium concentrations (severe hypokalemia, control and hyperkalemia). In all the graphs, the solid line (——) represents the solution that never came in contact with the tissue slice, the dotted line (.....) represents the conductivity of the solution after exposure to the tissue slices from weanling-aged (P15-P17) mice, and the dashed line (– –) represents the conductivity of the solution after exposure to tissue slices from neonatal-aged (P0–P2) mice.

hypokalemia. Furthermore, in neonates the increase in conductivity was significantly greater in hyperkalemic solution compared to moderate hypokalemic solution. This is different from the response observed in weanlings, in which the increase in conductivity was significantly smaller in hyperkalemic solution compared to moderate and hypokalemic solutions. In response to OGD, there was a greater increase in conductivity than that observed with the control solution. However, unlike the weanling data, in which the response to OGD was greater than that to moderate hypokalemia and hyperkalemia, in the neonate, there were no significant differences between the response to OGD and the responses to the three experimental potassium concentrations.

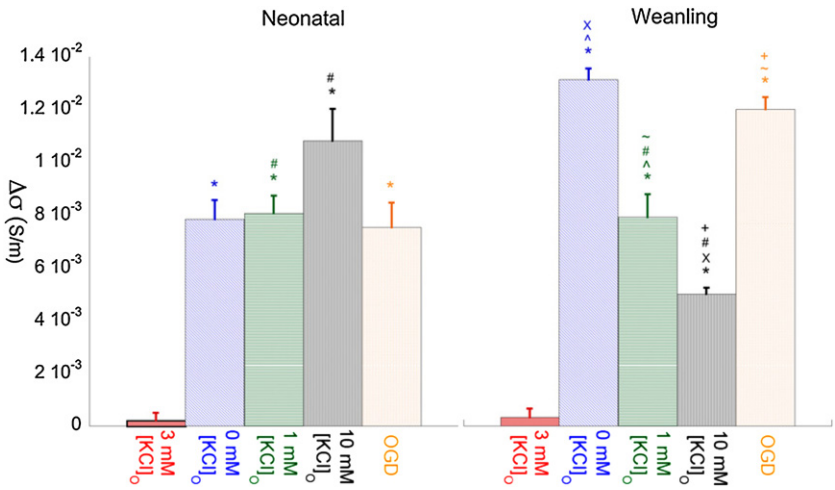

Figure 4. Changes in conductivity at 100 Hz of the various experimental solutions (control, severe and moderate hypokalemia, hyperkalemia and OGD) in which cortical tissue slices were bathed. Significant changes (denoted '*'; $p > 0.05$, $n = 6$–15) in conductivity with respect to the control condition (3 mM $[KCl]_O$) are seen in all experimental conditions over both age ranges tested (weanling and neonate). Additionally, significant changes ($p > 0.05$) between different pairings of pathological conditions are denoted by '^', '*X*', '#' '∼', and '+'.

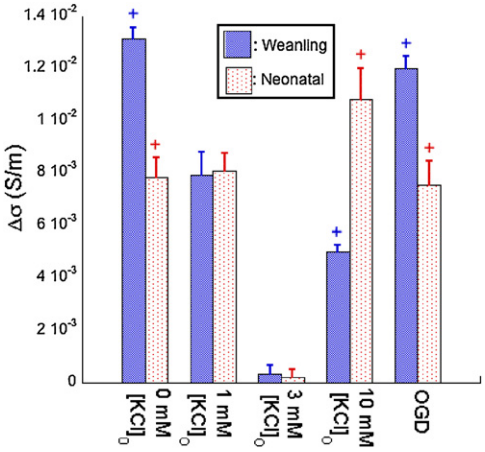

Figure 5. Change in conductivity (at 100 Hz) of solution due to exposure to tissue slice as a function of the mouse age. Significance ($P > 0.05$) between age groups within the same experimental condition is denoted by '+' above each bar.

In figure 5 we plotted the data corresponding to the change in conductivity to facilitate the comparison of the changes caused by each experimental solution between the two age ranges. Both severe hypokalemia and OGD produced significantly greater changes in weanlings compared to neonates. In contrast, the hyperkalemic solution produced a significantly greater increase in conductivity in neonates compared to weanlings.

4. Discussion

In this paper, the extracellular concentration of the potassium ion (K^+) in solutions in which cortical brain slices were bathed was altered (0 mM $[KCl]_O$, 1 mM $[KCl]_O$, 10 mM $[KCl]_O$) with respect to its normal physiological value. Under physiological conditions, the intracellular concentration of K^+ is many times greater than the extracellular CSF, which has a K^+ concentration that varies between 2.7 and 3.5 mM (Somjen 2002). Deviation from this range leads to biophysical changes to the cells that impair neural function. Low extracellular K^+ concentrations lead to hyperpolarization (Kuwabara *et al* 2002), increased intracellular Na^+ concentration (Korff *et al* 1984), and the induction of apoptosis (D'Mello *et al* 1993). Elevation of extracellular K^+ concentration has pathological consequences and is so lethal that a large exogenous dose of K^+ is used for capital punishment (Wong 2006). Under pathological conditions, such as epilepsy and stroke, the uppermost concentration limit of extracellular K^+ in the brain is approximately 12 mM (Heinemann and Lux 1977). During instances of head injury, the cortical extracellular potassium concentration can reach as high as 50 mM (Takahashi *et al* 1981).

In the present paper, we found that in cortical brain tissue from weanling mice there was a graded response to changes in the extracellular K^+ concentration. Severe hypokalemia led to significantly greater increases in extracellular conductivity compared to moderate hypokalemia or hyperkalemia. In contrast, there was no difference between the response to moderate and severe hypokalemia in neonates. Additionally, the response to hyperkalemia was significantly greater in neonates compared to weanlings. These results are consistent with the notion that compared to older mice, neonates have a limited ability to regulate the K^+ concentration in the CSF (Jones and Keep 1987).

In order for cells in the brain to maintain a constant extracellular concentration of potassium, the input of metabolic energy is essential. While the brain accounts for only a small percentage of total body weight, it accounts for nearly 20% of the body's total oxygen consumption; 70% of which is used to provide energy for the Na^+/K^+ ATPase (Edvinsson and Krause 2001), an enzyme that helps to maintain ionic concentration gradients across the plasma membranes of cells (Rossier *et al* 1987). Accordingly, the dysfunction of the Na^+/K^+ ATPase in brain cells leads to cellular death (Magyar *et al* 1994). Deprivation of cellular oxygen and glucose input leads to a reduction in intracellular ATP and an indirect shutdown of the Na^+/K^+ ATPase (Hertz 2008), potentially resulting in ionic hemostasis dysfunction (Thompson *et al* 2006) and necrotic cell death (Miyamoto and Auer 2000).

Accordingly, we hypothesized that a large increase in conductivity would occur during OGD. Interestingly, the increase in conductivity following OGD was significantly smaller in neonates compared to weanlings (figure 5). This difference likely corresponds to the observation that neonates possess a greater ability to withstand the OGD compared to older animals (Haddad and Donnelly 1990). Also of interest, the increases in extracellular conductivity in the severe hypokalemic and OGD groups were similar within each respective age group (figure 4). This observation may be due to the effect that both conditions have on the Na^+/K^+ ATPase. As the concentration of extracellular potassium diminishes, the efficacy of the ATPase is markedly decreased (Heidlage and Jones 1981). Similarly, as the amount of available ATP decreases during OGD, inhibition of Na^+/K^+ ATPase activity occurs (de Souza Wyse *et al* 2000). Therefore, it is possible that the state of dysfunction and poor cellular health in both cases is similar.

Since these measurements were conducted at low frequencies, it is quite likely that the electrical double layer effect dominates the measurements. The effect of this double layer impedance, which has been described by numerous researchers for decades, varies

dramatically with both ionic concentration and frequency (Mirtaheri *et al* 2005). Instead of viewing this double layer as a hindrance to collecting useful information, we actually used it to our advantage. We took painstaking measures, such as precisely maintaining the ionic concentrations presented in table 1, to ensure that the initial conductivities of baseline solutions were identical prior to the addition of the tissue. To ensure proper ionic concentrations in our solutions, we utilized both a conductivity meter and osmometer. Furthermore, instead of trying to remove the effect of the double layer impedance, we only concerned ourselves with evaluating the conductivity differences from these precise baseline solutions in order to use DS as a sensor. Thus, any variation from the initial conductivity of the solution represents the response of the tissue to the insult.

While the change in extracellular solution conductivity is clearly frequency-dependent, it is likely that the change is also time-dependent. In pathological conditions such as ischemia (OGD), there is a rapid and punctuated rise in extracellular potassium concentration within minutes of the OGD onset (Hansen 1985). Subsequently, the extracellular potassium concentration plateaus around 50 mM for the remainder of the ischemic insult. Given that our exposure duration was 20 min, it is possible that a large flux of potassium ions could have contributed to the extracellular solution conductivity.

5. Conclusions

Since both necrotic and apoptotic cellular death mechanisms involve a net efflux of ions from the dying cell, evaluation of the extracellular ion profile may provide useful insight into the health and vitality of neural tissue. While methods such as double-barreled ion-selective microelectrodes measure changes in the concentration of a single ionic species, they lack the ability to simultaneously assess the contribution of several different ionic species. In this paper, we utilized DS, which allows for the measurement of the net change in number of all charged particles in solution (i.e. a solution's conductivity).

Acknowledgment

This research was funded by National Institute of Health grant # 2R44NS048682-02A1.

References

Akhtari M, Salamon N, Duncan R, Fried I and Mathern G W 2006 Electrical conductivities of the freshly excised cerebral cortex in epilepsy surgery patients; correlation with pathology, seizure duration, and diffusion tensor imaging *Brain Topogr.* **18** 281–90

Bordi F, Cametti C and Colby R H 2004 Dielectric spectroscopy and conductivity of polyelectrolyte solutions *J. Phys.: Condens. Matter* **16** R1423–63

Bortner C D, Hughes F M and Cidlowski J A 1997 A primary role for K+ and Na+ efflux in the activation of apoptosis *J. Biol. Chem.* **272** 32436–42

Bot C and Prodan C 2009 Probing the membrane potential of living cells by dielectric spectroscopy *Eur. Biophys. J.* **38** 1049–59

Caduff A, Dewarrat F, Talary M, Stalder G, Heinemann L and Feldman Y 2006 Non-invasive glucose monitoring in patients with diabetes: a novel system based on impedance spectroscopy *Biosens. Bioelectron.* **22** 598–604

Cametti C, Fratoddi I, Venditti I and Russo M V 2011 Dielectric relaxations of ionic thiol-coated noble metal nanoparticles in aqueous solutions: electrical characterization of the interface *Langmuir* **27** 7084–90

Chen T and Hefter G 2003 Dielectric spectroscopy of aqueous solutions of KCl and CsCl *J. Phys. Chem.* A **107** 4025–31

Coury L 1999 Conductance measurements, part 1: theory *Curr. Sep.* **18** 91–6

D'Mello S R, Galli C, Ciotti T and Calissano P 1993 Induction of apoptosis in cerebellar granule neurons by low potassium: inhibition of death by insulin-like growth factor I and cAMP *Proc. Natl Acad. Sci.* **90** 10989–93

de Souza Wyse A T, Streck E l L, Worm P, Wajner A, Ritter F and Netto C A 2000 Preconditioning prevents the inhibition of Na+, K+-ATPase activity after brain ischemia *Neurochem. Res.* **25** 971–5

Di Biasio A and Cametti C 2011 On the dielectric relaxation of biological cell suspensions: the effect of the membrane electrical conductivity *Colloids Surf.* B **84** 433–41

Dobiszewski K F, Shaker M R, Deek M P, Prodan C and Hill A A 2011 Design and implementation of a novel superfusion system for *ex vivo* characterization of neural tissue by dielectric spectroscopy (DS) *Physiol. Meas.* **32** 195–207

Du C, Yu M, Volkow N D, Koretsky A P, Fowler J S and Benveniste H 2006 Cocaine increases the intracellular calcium concentration in brain independently of its cerebrovascular effects *J. Neurosci.* **26** 11522–31

Edvinsson L and Krause D N 2001 *Cerebral Blood Flow and Metabolism* (Baltimore, MD: Lippincott, Williams & Wilkins)

Egot-Lemaire S, Pijanka J, Sulé-Suso J and Semenov S 2009 Dielectric spectroscopy of normal and malignant human lung cells at ultra-high frequencies *Phys. Med. Biol.* **54** 2341

Gersing E 1998 Impedance spectroscopy on living tissue for determination of the state of organs *Bioelectrochem. Bioenerg.* **45** 145–9

Gheorghiu M and Gersing E 2002 Revealing alteration of membrane structures during ischemia using impedance spectroscopy *Songklanakarin J. Sci. Technol.* **24** 777–84

Haddad G G and Donnelly D F 1990 O_2 deprivation induces a major depolarization in brain stem neurons in the adult but not in the neonatal rat *J. Physiol.* **429** 411–28

Hansen A J 1985 Effect of anoxia on ion distribution in the brain *Physiol. Rev.* **65** 101–48

Heidlage J F and Jones A W 1981 The kinetics of ouabain-sensitive ionic transport in the rabbit carotid artery *J. Physiol.* **317** 243–62

Heinemann U and Lux H D 1977 Ceiling of stimulus-induced rises of extracellular potassium concentration in the cerebral cortex of cat *Brain Res.* **120** 231–49

Hertz L 2008 Bioenergetics of cerebral ischemia: a cellular perspective *Neuropharmacology* **55** 289–309

Hitoshi S, Takeshi S, Ching-Chou W, Tomoyuki Y, Tomokazu M, Hiroyoski H, Masaki Y, Hiroyuki A and Hiroshi Y 2005 Oxygen permeatbility for poly(Dimethylsiloxane) (PDMS) characterized by feedback-mode scanning electrochemical microscopy *Chem. Sensors* **21** 49–51

Hodgkin A L and Keynes R D 1955 The potassium permeability of giant nerve fibre *J. Physiol.* **128** 61–88

Husted R F and Reed D J 1977 Regulation of cerebrospinal fluid bicarbonate by the cat choroid plexus *J. Physiol.* **267** 411–28

Jones H C and Keep R F 1987 The control of potassium concentration in the cerebrospinal fluid and brain interstitial fluid of developing rats *J. Physiol.* **383** 441–53

Kettenmann H, Sonnhof U and Schachner M 1983 Exclusive potassium dependence of the membrane potential in cultured mouse oligodendrocytes *J. Neurosci.* **3** 500–5

Korff J M, Siebens A W and Gill J R J 1984 Correction of hypokalemia corrects the abnormalities in erythrocyte sodium transport in Bartter's syndrome *J. Clin. Investig.* **74** 1724–9

Kuwabara S, Kanai K, Sung J-Y, Ogawara K, Hattori T, Burke D and Bostock H 2002 Anoxal hyperpolarization associated with acute hypokalemia: multiple excitability measurements as indicators of the membrane potential of human axons *Muscle Nerve* **26** 283–7

Lee R M, Choi H, Shin J-S, Kim K and Yoo K-H 2009 Distinguishing between apoptosis and necrosis using a capacitance sensor *Biosens. Bioelectron.* **24** 2586–91

Magyar J P, Bartsch U, Wang Z-Q, Howells N, Aguzzi A, Wagner E F and Schachner M 1994 Degeneration of neural cells in the central nervous system of mice deficient in the gene for the adhesion molecule on glia, the $\beta 2$ subunit of murine Na,K-ATPase *J. Cell Biol.* **127** 835–45

Mirtaheri P, Grimnes S and Martinsen Ø G 2005 Electrode polarization impedance in weak NaCl aqueous solutions *IEEE Trans. Biomed. Eng.* **52** 2093–9

Miyamoto O and Auer R N 2000 Hypoxia, hyperoxia, ischemia, and brain necrosis *Neurology* **54** 362–71

Morrison B M 2008 *Cerebrospinal Fluid in Clinical Practice* ed D N Irani (Philadelphia, PA: Saunders Elsevier) p 12

Müller M and Somjen G G 2000 Na+ and K+ concentrations, extra- and intracellular voltages, and the effect of TTX in hypoxic rat hippocampal slices *J. Neurophysiol.* **83** 735–45

Murai Y, Ishibashi H, Koyama S and Akaike N 1997 Ca2+−Activated K+ currents in rat locus coeruleus neurons induced by experimental ischemia, anoxia, and hypoglycemia *J. Neurophysiol.* **78** 2674–81

O'Rourke A P, Lazebnik M, Bertram J M, Converse M C, Hagness S C, Webster J G and Mahvi D M 2007 Dielectric properties of human normal, malignant and cirrhotic liver tissue: *in vivo* and *ex vivo* measurements from 0.5 to 20 GHz using a precision open-ended coaxial probe *Phys. Med. Biol.* **52** 4707–19

Prodan C, Mayo F, Claycomb J R, Miller J H and Benedik M J 2004 Low-frequency, low-field dielectric spectroscopy of living cell suspensions *J. Appl. Phys.* **95** 3754–6

Remillard C V and Yuan J X-J 2004 Activation of K+ channels: an essential pathway in programmed cell death *Am. J. Physiol.: Lung Cell. Mol. Physiol.* **286** L49–67

Ron A, Singh R R, Fishelson N, Shur I, Socher R, Benayahu D and Shacham-Diamand Y a 2008 Cell-based screening for membranal and cytoplasmatic markers using dielectric spectroscopy *Biophys. Chem.* **135** 59–68

Rossier B C, Geering K and Kraehenbuhl J P 1987 Regulation of the sodium pump: how and why? *Biochem. Sci.* **12** 483–7

Santhakumar V, Voipio J, Kaila K and Soltesz I 2003 Post-traumatic hyperexcitability is not caused by impaired buffering of extracellular potassium *J. Neurosci.* **23** 5865–76

Schaefer M, Gross W, Ackemann J and Gebhard M 2002 The complex dielectric spectrum of heart tissue during ischemia *Bioelectrochemistry* **58** 171–80

Schmid G, Neubauer G and Mazal P R 2003 Dielectric properties of human brain tissue measured less than 10 h postmortem at frequencies from 800 to 2450 MHz *Bioelectromagnetics* **24** 423–30

Somjen G G 2002 Ion regulation in the brain: implications for pathophysiology *Neuroscientist* **8** 254–67

Takahashi H, Manaka S and Sano K 1981 Changes in extracellular potassium concentration in cortex and brain stem during the acute phase of experimental closed head injury *J. Neurosurg.* **55** 707–17

Thompson R J, Zhou N and MacVicar B A 2006 Ischemia opens neuronal gap junction hemichannels *Science* **312** 924–7

van Mil H, van Heukelomb J S and Bierc M 2003 A bistable membrane potential at low extracellular potassium concentration *Biophys. Chem.* **106** 15–21

Warny M and Kelly C P 1998 Monocytic cell necrosis is mediated by potassium depletion and caspase-like proteases *Am. J. Physiol.: Cell. Physiol.* **276** C717–24

Wong J R 2006 Lethal injection protocols: the failure of litigation to stop suffering and the case for legislative reform *Temple J. Sci. Technol. Environ. Law* **25** 263